RSC Publishing Faraday Discussions

Quantum and Classical IR Spectra of (HCOOH)2, (DCOOH)2 and (DCOOD)2 using Ab Initio Potential Energy and Dipole Moment Surfaces

Journal:	*Faraday Discussions*
Manuscript ID	FD-ART-04-2018-000077.R1
Article Type:	Paper
Date Submitted by the Author:	27-Apr-2018
Complete List of Authors:	Chen, Qu; Emory University, Chemistry Bowman, Joel; Emory University, Chemistry

Journal Name

ARTICLE TYPE

Cite this: DOI: 10.1039/xxxxxxxxxx

Quantum and Classical IR Spectra of $(HCOOH)_2$, $(DCOOH)_2$ and $(DCOOD)_2$ using Ab Initio Potential Energy and Dipole Moment Surfaces

Chen Qu and Joel M. Bowman*

Received Date
Accepted Date

DOI: 10.1039/xxxxxxxxxx

www.rsc.org/journalname

The accurate quantum mechanical description of the vibrational dynamics and IR spectra of molecules is illustrated here for the formic acid dimer, $(HCOOH)_2$ and isotopologues $(DCOOH)_2$ and $(DCOOD)_2$ in full dimensionality. The calculations make use of recent full-dimensional *ab initio* potential energy and dipole moment surfaces and are done with the code MULTIMODE. IR spectra are reported for the three dimers and also compared to available experimental spectra. In addition, standard classical and "semiclassially prepared" quasiclassical molecular dynamics calculations of the IR spectra of these complexes are reported and compared to the quantum spectra and also experiment. These comparisons indicate good accuracy of the MD spectra for sharp bands but not for the complex O-H stretch band, where the complex molecular dynamics band is upshifted from experiments by roughly 300 cm^{-1}. For the the fully deuterated dimer $(DCOOD)_2$, the quantum spectral band for O-D stretch sharpens relative to the O-H spectral bands in $(HCOOH)_2$ and $(DCOOH)_2$; however, the molecular dynamics OD stretch band does not exhibit this sharpening.

1 Introduction

The accurate quantum treatment of vibrational, ro-vibrational energies and IR spectra of small molecules, i.e., 3–5 atoms, has seen major progress in the past decade or so. Recent reviews have appeared, [1–5] which can be consulted for the breadth of this progress, which is most substantial for tetratomic molecules and non-covalent complexes. Accurate quantum calculations of the vibrational energies of methane have also been reported [4]; however, in general 5-atom molecules and complexes are still a challenge for "exact" quantum treatments.

The terms "exact" and "accurate" used above deserve at least some brief discussion, as there are no universally accepted definitions of these terms. Here is what we mean in the present context. The components of an accurate, first-principles computational treatment of vibrational dynamics are, an accurate potential energy surface (PES), an "exact" or nearly "exact" solution of the "exact" Schroedinger equation and, for the IR spectrum, an accurate dipole moment surface (DMS). There are challenges associated with each of these ingredients.

Starting with the potential, it is now generally accepted that the coupled cluster method, with at least a perturbative treatment of triple excitations, is needed for accurate energies. These energies are needed at a sufficient number of nuclear configurations to obtain a fit that is precise, at least at the expected level of the accuracy of the electronic energies themselves. These days this level is of the order of 1-10 cm^{-1} and generally closer to the upper end of this range. The direct use of electronic energies in vibrational calculations, that is without the use of fitted potential energy surface, is of course possible; however, rarely feasible, without also making some approximation to the size of the grids needed to solve the Schroedinger equation. There has been great progress in developing highly precise, high-dimensional representation of tens of thousands of electronic energies, and a recent review we wrote on this can be consulted for further details of this progress. [6] Predating this approach, *ab initio*-based force-fields, i.e., multinomial, direct-product representations of potentials, have been widely used very effectively. These and sophisticated variations of force fields, now referred to a "sum-of-products" representation are most effective in representing a limited region of configuration space, e.g., the region around a minimum on the potential.

Less attention has been paid to representing the dipole moment surface, which is a vector quantity of course and which is in principle the same dimensionality as the corresponding PES. We have proposed and used permutationally invariant representations of the dipole moment surface. [7,8]

Department of Chemistry and Cherry L. Emerson Center for Scientific Computations, Emory University, Atlanta, Georgia 30322, USA. E-mail: jmbowma@emory.edu

Finally, there is the matter of solving the nuclear Schroedinger equation, once the PES (and DMS) is in hand. There are numerous approaches for this and the reviews mentioned in the first paragraph described most of these. Another family of methods is the so-called dynamical approach that uses the autocorrelation function from dynamics simulations to compute the spectrum.[9–12] Here we use the vibrational self-consistent field/vibrational configuration interaction (VSCF/VCI) method[13,14] implemented in the code MULTIMODE[15–17] and classical molecular dynamics (MD) for this purpose and relevant details of these two approaches are given below for the subject application of this paper, the vibrational dynamics and IR spectrum of the formic acid dimer (FAD).

The FAD (and isotopologues) is the smallest example of a carboxylic acid dimer, and therefore is one of the mostly intensively studied hydrogen-bonded dimers. However, with 10 atoms, it still presents a formidable challenge to theory, due to the high dimensionality for rigorous quantum approach to solve the nuclear Schroedinger equation. In addition, there are two equivalent double hydrogen-bond minima, connected by a transition state of the double-hydrogen transfer, and this signals possible complex vibrational dynamics. In fact, this double-hydrogen transfer gives rise to a small tunneling splitting, which is only about 0.015 cm^{-1},[18,19] and possibly contributes, at least indirectly, to some complex bands in the IR (and Raman) spectrum.[18–29]

The tunneling splitting and the dynamics of the double-proton transfer have been studied theoretically.[30–48] Recently, major progress has been made in the calculation of the ground-state tunneling splitting in full dimensionality,[48] using our recent full-dimensional *ab initio* PES.[47] The calculated splitting, 0.014 cm^{-1}, is in good agreement with experimental value of roughly 0.015 cm^{-1}, and this demonstrates the accuracy of our PES. In this work, this PES is used in calculations of vibrational energies and IR spectra of FAD and its isotopologues, with the focus on the complex O-H(D) stretch bands.

The experimental IR spectrum has been reported numerous times, notably in the C-O, C-H and O-H stretch regions of the spectrum.[20–24] Theoretical work on the vibrational spectrum is also extensive, beginning with *ab initio* double-harmonic calculations in 1987.[49] Other early work used reduced-dimensionality calculations, due to the large degree-of-freedom (dof) of the molecule.[30,32,34] Recent theoretical work focused on C-H and O-H stretch regions of the IR spectrum, owing to the extreme complexity of this experimental band. Vener et al.[34] carried out a 3-dof study of the double proton transfer, and reported that the splitting of the IR-active antisymmetric OH stretch fundamental is 70 cm^{-1}, and this may be responsible for the width of the O-H stretch band. Florio et al.[26] developed full and reduced dimensionality cubic force fields expanded around one minimum, using B3LYP density functional. These cubic force constants, together with linear dipole moments, were used to simulate the spectrum of FAD. When forces constants that couple the CH and OH stretches with low-frequency modes were included, theory could be brought into reasonable agreement with experiment. More recently, Matanović and Došlić[50] used both second-order perturbative treatment and 2- and 3-mode vibrational configuration interaction calculations based on B3LYP method. The conclusions were that coupling to low-frequency dimer and rocking modes and Fermi resonances contributed to the width of the band, but had only a minor effect on the frequency of the band maximum, while coupling to the symmetric OH stretch causes the red-shift of the band. Pitsevich et al.[51] performed VPT2 calculations of the fundamentals of FAD and developed extended 1d and 2d potential energy surfaces using B3LYP/cc-pVTZ calculations to study anharmonic effects in the C-H and O-H stretches. However, the IR spectrum was not simulated in these calculations. All of these calculations have made compromises in both the electronic structure theory and the degree of mode coupling. In addition, these calculations were restricted to a single minimum, with the exception of the work by Vener et al.

As noted above, we recently reported a full-dimensional PES,[47] which was based on CCSD(T)-F12a electronic energies. More recently, we reported a full-dimensional MP2-based DMS, which was used with the PES in 15-dof VSCF/VCI calculations of the IR spectrum of FAD.[52] Here, we use these potential and dipole moment surfaces in full-dof (24 modes) VSCF/VCI calculations of the IR spectrum of FAD and its isotopologues. In addition, we assess and report the accuracy of "*ab initio* molecular dynamics" (AIMD) calculations of these spectra. In the present case "*ab initio*" refers to the direct evaluation of the potential, the gradient of the potential, and the dipole moment "on the fly." Given that a single CCSD(T)-F12 calculation of the FAD using haTZ basis (aVTZ for C and O, and VTZ for H) takes roughly 40 minutes on an 8-core cpu, a "direct" approach is unfeasible. Nevertheless, with the help of our PES and DMS, these MD simulations become feasible.

We are motivated to perform these MD calculations for general and specific reasons. The general motivation is that AIMD is widely used to obtain the IR spectra of larger molecules, clusters, etc., owing to the difficulties in accurate quantum calculations for such systems. Therefore, it's necessary to access the accuracy of the MD approach in the calculation of IR spectrum, by comparing the results with more rigorous quantum calculations and the experiment. The specific motivation is that MD simulations of the IR spectra of $(HCOOH)_2$ and $(DCOOH)_2$, using model potential and dipole moment surfaces, were recently reported.[24] The PES is an example of the "MMPT" force field for proton transfer, developed by Meuwly and co-workers, in which limited *ab initio* data is used to determine some of the parameters in the functional form of the PES. For FAD, MMPT-MP2 and MMPT-B3LYP force fields were developed. The DMS is a fixed charge model, using B3LYP atomic charges at the double proton barrier configuration. Molecular dynamics simulations of the location of the complex OH band using these produced results that were upshifted from experiment by several hundred wavenumbers (in fact in agreement with the present MD results, see Section 3). Interestingly, the MMPT-MP2 PES has a barrier height of 8.2 kcal/mol, in good agreement with the barrier height of 8.2 kcal/mol of the present PES. Then these authors adjusted the PESs, mainly by changing the barrier of double-proton transfer, to produce a position of this band in good agreement with experiment. The "optimized" barrier for the MMPT-B3LYP force field equals 5.1 kcal/mol and the

one for the MMPT-MP2 force field equals 7.2 kcal/mol. The authors thus concluded that the barrier for the double proton transfer is between 5 and 7 kcal/mol. (Even with this adjustment to the barrier height, it is worth noting that the fixed-charged dipole model produced intensities for a number of sharp bands that are in poor agreement with experiment.) This procedure to bring the MD spectrum in the complex O-H stretch region into agreement with the room-temperature experimental spectra by varying the barrier height assumes that the MD description of this band is sufficiently accurate to provide a reliable estimate of the barrier height. We examine this assumption specifically here. However, the fact that the "optimized" barrier is significantly lower than directly calculated CCSD(T) one already raises some doubts about this assumption.

The VSCF/VCI calculations were done with the code MULTIMODE,[16,17] which uses the exact Watson Hamiltonian[53] and an efficient *n*-mode representation of the potential energy (and dipole moment) surface.[15] These calculations just considered one single minimum so they do not describe the proton transfer. We discuss the possible influence of this double-proton transfer, which we conclude is negligible for the present comparison with experiments, later.

The MD simulations are standard constant-energy (NVE) ones, where the total energy corresponds to a temperature of 300 K, and additional ones in which harmonic zero-point energy is given to each of the normal modes. The latter follows the "semiclassically prepared molecular dynamics" approach suggested and tested on *trans*-HONO.[10] But we denoted it as "quasiclassical molecular dynamics" (QCMD) in a recent paper on small protonated water clusters.[54] Since the procedure is semiclassical, it is subject to the well-known "zero-point energy leak," which can cause artificial broadening of spectral bands. However, the hope is that this semiclassical approach is able to capture the anharmonic effects much better than the NVE one.

Section 2 briefly describes the PES and DMS, and provides theories and computational details of the VSCF/VCI and MD calculations. Section 3 presents the results of the computations and discussions on these results. A summary and conclusions are given in Section 4.

2 Computational Details

2.1 Potential Energy and Dipole Moment Surfaces

The PES and DMS are linear least-squares fits to 13475 *ab initio* CCSD(T)-F12a electronic energies and MP2 dipole moments, using permutationally invariant polynomials as the fitting basis, so that the PES and DMS are invariant when two atoms of the same type are permuted. The details of the fit and the properties of them can be found in refs. 47 and 52. It is worth mentioning that the barrier height of the double proton transfer is 8.2 kcal/mol in the fitted PES, and it agrees well with the CCSD(T)/aV5Z benchmark[45] value of 8.3 kcal/mol.

2.2 MULTIMODE calculations

The VSCF/VCI calculations were performed with the MULTIMODE software,[16,17] which determines the eigenvalues and eigenfunctions of the Watson Hamiltonian[53] in normal coordinates $\boldsymbol{Q}$ with $J=0$ in the present calculations. Calculations with J >0 are computationally very demanding compared to those for J $=0$, reported here. This would certainly be a goal for the future; however, for the present, our goal is to locate the major bands in the IR spectra.

The kinetic energy operator of the Watson Hamiltonian for $J=0$ is given by

$$\hat{T}=\frac{1}{2}\sum_{\alpha,\beta}\hat{\pi}_\alpha\mu_{\alpha\beta}\hat{\pi}_\beta-\frac{1}{8}\sum_\alpha\mu_{\alpha\alpha}-\frac{1}{2}\sum_{k=1}^{N}\frac{\partial^2}{\partial Q_k^2}, \tag{1}$$

where N is the number of normal modes in the molecule, $\mu_{\alpha\alpha}$ is the inverse of the effective moment of inertia tensor, and

$$\hat{\pi}_\alpha=-i\sum_{k,l=1}^{N}\zeta_{k,l}^{\alpha}Q_k\frac{\partial}{\partial Q_l} \tag{2}$$

are vibrational angular momentum terms and $\zeta_{k,l}^{\alpha}$ are Coriolis coupling constants.

One key aspect of the code is the *n*-mode representation (*n*MR) of the potential and the inverse of the effective moment of inertia tensor.[15] In the *n*-mode representation the potential $V(\boldsymbol{Q})$ is given by

$$V(\boldsymbol{Q})=V^{(0)}+\sum_i V_i^{(1)}(Q_i)+\sum_{ij}V_{ij}^{(2)}(Q_i,Q_j)+\sum_{ijk}V_{ijk}^{(3)}(Q_i,Q_j,Q_k)+\cdots \tag{3}$$

MULTIMODE currently truncates this representation at a maximum value of $n=6$. Based on many applications, we have determined that a four-mode representation is generally sufficient to obtain converged eigenvalues to one wavenumber or less. This level of mode representation leads to at most four-dimensional numerical quadratures. There are $N!/(N-n)!n!$ sets of grids for a given n. So for example of FAD, where $N=24$, there are 24 sets of one-mode grids, 276 two-mode grids, 2024 three-mode grids, and 10626 four-mode grids.

In the VSCF step, the total vibrational wavefunction is assumed to be a direct product of one-mode functions, and the optimal one-mode functions are found using the standard self-consistent field scheme. A VSCF ground state and a series of virtual states can be obtained from the VSCF calculation, and these states are used as basis functions for the VCI calculation. The VCI wavefunction can be expressed as

$$\psi_L=\sum_{i=1}^{K}c_i^{(L)}\phi_i, \tag{4}$$

where the basis, $\{\phi\}$, consists of direct-product, virtual states of the VSCF Hamiltonian and K is the size of the basis. The CI coefficients, c_i, can be used for the assignment of the spectrum.

For the VCI calculation, the size of the full-CI Hamiltonian matrix is m^N, where m is the number of basis functions per mode, and N is the number of modes. So constraints must be added to the excitation space in order to reduce the size of the matrix. First MULTIMODE restricts the number of modes that can be excited simultaneously. The maximum allowed value is 6, but we found that 4 is adequate in most cases to achieve good convergence. In

addition, the maximal quanta of excitation for each mode and the sum of quanta are also restricted. With these constraints, the size of the final CI matrix is of order ∼10000. When the molecule has symmetry, it can also be exploited so that the matrix becomes block-diagonal, and each block is of smaller size.

The IR intensities were calculated using

$$I_{f\leftarrow i} = \frac{8\pi^3 N_A}{3hc(4\pi\varepsilon_0)} \nu_{f\leftarrow i} \sum_{\alpha=x,y,z} \left| \int \psi_i(\boldsymbol{Q}) \mu_\alpha(\boldsymbol{Q}) \psi_f(\boldsymbol{Q}) \right|^2, \quad (5)$$

where N_A is the Avogadro's number, h is the Planck constant, c is the speed of light, ε_0 is the vacuum permittivity, $\nu_{f\leftarrow i}$ is the wavenumber of the transition, and the wavefunctions $\psi_i(\boldsymbol{Q})$ are obtained from the VSCF/VCI calculations. Since the absolute intensities of the experiments are not available, we just scale each spectrum so that the height of the most intense line (the C=O stretch at about 1750 cm^{-1}) is 1. The absolute intensities can be calculated using eqn. 5 and these are available to the interested reader by contacting the authors.

We were not aiming at high-resolution spectra of FAD and its isotopologues, so we did not consider the small tunneling effect and the VSCF/VCI calculations were performed at one of the equivalent minima. This will be discussed in Section 3. The calculations were similar to the ones we recently reported,[52] except that we coupled all the normal modes (24 modes) in the current calculation. To make the calculations computationally feasible, a 4-mode representation of the FAD potential and a 3-mode representation of the dipole moment were used in order to evaluate the matrix elements efficiently. We also constrained the excitation space in the VCI calculation, in order to limit the size of the final Hamiltonian matrix. We only allowed simultaneous excitation of at most 4 modes, and the excitation cannot exceed 6 quanta for each mode, and furthermore, the sum of quanta of all the modes cannot exceed 6. This is a relatively small excitation space, but for a 24-mode system, increasing the excitation space further is almost infeasible. In addition to the restrictions on excitation in VCI, the C_{2h} point-group symmetry was exploited to set up a 4-block Hamiltonian matrix, each of which is of order 20,000.

Many standard convergence tests, including the n-mode representation of the potential, the size of basis functions, and the excitation space in the VCI calculation, were performed and we estimate that the calculated spectra (for a given number of coupled modes) shown are converged to within roughly 10 cm^{-1} or less. As an additional evidence for good convergence of the VSCF/VCI calculations, the ground state energies in these calculations, 15340 cm^{-1} for $(HCOOH)_2$, 13947 cm^{-1} for $(DCOOH)_2$, and 12469 cm^{-1} for $(DCOOD)_2$, agree very well with the zero-point energies of the three isotopologues obtained from diffusion Monte Carlo calculations, which are 15337 ± 7 cm^{-1} for $(HCOOH)_2$, 13944 ± 9 cm^{-1} for $(DCOOH)_2$, and 12470 ± 6 cm^{-1} for $(DCOOD)_2$, respectively. Thus, we believe the spectra obtained using the full 24 modes should be reasonably well-converged, at least for the purpose of graphical comparison to experimental spectra.

2.3 Molecular dynamics calculations

The IR absorption coefficient is given by

$$\alpha(\omega) = Q(\omega) \frac{4\pi^2 \omega}{3cV\hbar} \left(1 - e^{-\beta\hbar\omega}\right) I(\omega), \quad (6)$$

where V is the volume, c is the speed of light, and $\beta = 1/k_B T$. $I(\omega)$ is the spectral line shape function, which is the Fourier transform of the dipole-dipole autocorrelation function:

$$I(\omega) = \frac{1}{2\pi} \int_{-\infty}^{+\infty} e^{-i\omega t} \langle \boldsymbol{\mu}(t) \cdot \boldsymbol{\mu}(0) \rangle dt, \quad (7)$$

where the "$\langle \ldots \rangle$" means the ensemble average. This dipole-dipole autocorrelation function can be obtained using classical dynamics simulations. $Q(\omega)$ is the quantum correction factor, and a typical choice is

$$Q(\omega) = \frac{\beta\hbar\omega}{1 - e^{-\beta\hbar\omega}}, \quad (8)$$

which makes the line shape function satisfy the detailed balance condition. Therefore, the final expression to calculate the spectra using dipole autocorrelation function is given by

$$\alpha(\omega) = \frac{2\pi\beta\omega^2}{3Vc} \int_{-\infty}^{+\infty} e^{-i\omega t} \langle \boldsymbol{\mu}(t) \cdot \boldsymbol{\mu}(0) \rangle dt. \quad (9)$$

Note that Eq. 9 is based on MD simulations using thermostats, but in this work, as we will show next, it should be ω rather than ω^2 in the prefactor, due to the method of initial condition sampling we employed.

In this work, a special type of classical NVE simulations was used. In these calculations, instead of distributing energy randomly to each atom as the initial condition, we assigned energy to each normal mode based on its harmonic frequency. To be specific, normal mode i receives $\alpha\hbar\omega_i$ as its initial energy, where α is a factor that depends on the target total energy of the molecule, and ω_i is the harmonic frequency of that mode. Here we consider two target total energies: the energy that corresponds to 300 K (the room temperature, at which most of the classical MD is performed), and the harmonic zero-point energy of the molecule.[10] The latter is termed as "QCMD" in this article, and in this case, α is 0.5.

Because of this sampling method, the energy in each normal mode is proportional to its harmonic frequency, in contrast to thermostat MD, where the energy in each normal mode is the same ($k_B T$ after equilibration), according to equipartition theorem. Therefore, an ω weight is already carried by the dipole-dipole autocorrelation function in our method, so it should be ω rather than ω^2 in the prefactor in Eq. 9. The standard procedures of normal mode sampling, described in ref. 55, were used to prepare the initial conditions for the MD simulations. Briefly, the momentum (P_i) and position (Q_i) in normal-mode coordinates are generated based on

$$Q_i = \left(\sqrt{2E_i}/\omega_i\right) \cos\phi, \quad (10)$$

$$P_i = -\sqrt{2E_i} \sin\phi, \quad (11)$$

where E_i is the energy to be deposited into mode i, and ϕ is a

random number drawn from a uniform distribution on $(0, 2\pi]$. For QCMD, $E_i = \frac{1}{2}\hbar\omega_i$, while for trajectories at 300 K, $E_i = \alpha\hbar\omega_i$, where α is 0.161 for $(HCOOH)_2$, 0.177 for $(DCOOH)_2$, and 0.198 for $(DCOOD)_2$, so that the total energy in the molecule is 5004 cm^{-1}, corresponding to the 300 K temperature.

One hundred trajectories were performed for the 300 K simulations, and 600 trajectories for QCMD. In some QCMD trajectories the dimer dissociates so these were not included when calculating the spectrum, and trajectories in which the double-proton transfer occurred were not included, either. In total, 293 QCMD trajectories were used to compute the IR spectrum of $(HCOOH)_2$, 439 for $(DCOOH)_2$, and 522 for $(DCOOD)_2$. Each trajectory was propagated for 12 ps, and the velocity Verlet integrator with a time step of 0.06 fs was used for all the trajectories. The standard dipole-dipole autocorrelation function $C(t) = \langle \boldsymbol{\mu}(t) \cdot \boldsymbol{\mu}(0) \rangle$ was recorded for each, then averaged over the set of trajectories, and finally Fourier transformed to obtain the spectra.

3 Results and Discussion

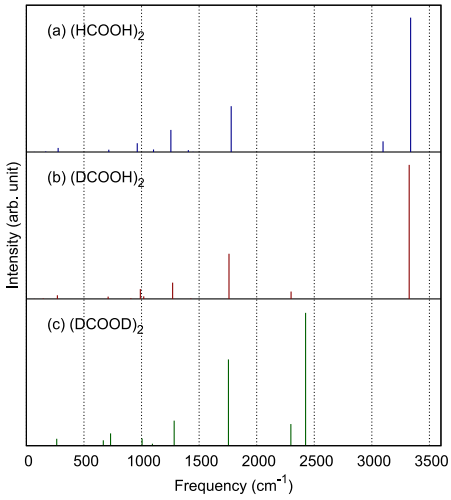

Fig. 1 Double harmonic spectra of the three isotopologues of the FAD.

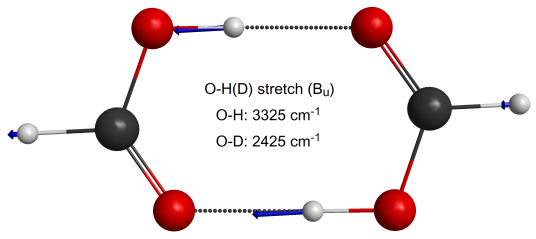

Fig. 2 The intense O-H(D) stretch mode of the formic acid dimer.

To begin, consider the double harmonic spectra of $(HCOOH)_2$, $(DCOOH)_2$, and $(DCOOD)_2$, obtained from our PES and DMS, in Figure 1. The stick locations are of course just the harmonic normal mode frequencies. The intense O-H stretch in $(HCOOH)_2$ and $(DCOOH)_2$ is at 3325 cm^{-1} and for $(DCOOD)_2$ the corresponding line for the O-D stretch is at 2425 cm^{-1}, and this mode is shown in Figure 2. We focus on these intense features in this spectrum because they emerge as complex bands in the calculated spectra reported below. Even at this simple level of treatment of the O-H stretch there is a hint of strong coupling of this mode. This comes from noting that in isolated formic acid the experimental, and thus anharmonic, O-H stretch is at 3570 cm^{-1},[56] more than 200 cm^{-1} higher than the harmonic O-H stretch in the dimer. Clearly, the double hydrogen bonding in the dimer strongly perturbs the O-H stretch, as has been noted previously in the FAD literature.

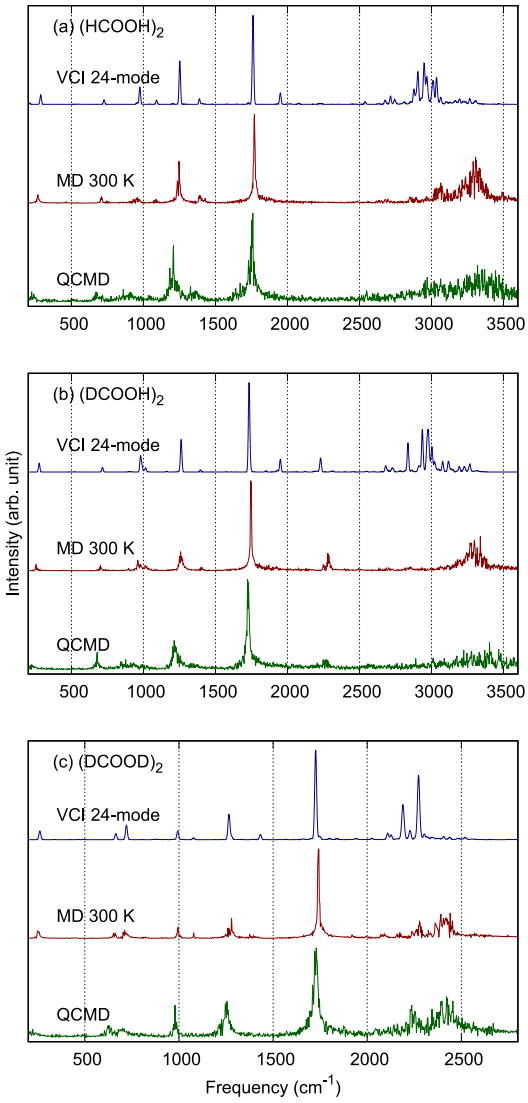

Fig. 3 Comparison of the IR spectrum of (a) $(HCOOH)_2$, (b) $(DCOOH)_2$, and (c) $(DCOOD)_2$ from quantum VSCF/VCI and indicated classical MD calculations.

Figure 3 shows the comparison between the VSCF/VCI spectrum with the AIMD one for $(HCOOH)_2$, $(DCOOH)_2$, and $(DCOOD)_2$, respectively. For transitions below 1800 cm^{-1}, the quantum and AIMD spectra agree very well, on both positions and intensities, while for the C-H(D) and O-H(D) stretch bands, the AIMD method overestimates the frequency by 200–300 cm^{-1}. This upshift of the stretch band in the AIMD spectra is well understood. In classical simulations, 300 K corresponds to 208 cm^{-1} per dof, which is a small amount of energy for the high-frequency

modes. As a consequence, the MD trajectories basically just sample the harmonic part of the potential. So the positions of the stretch bands are close to their harmonic frequencies. Interestingly, when QCMD is applied, we don't observe any down-shifts of the stretch bands, which is not expected. In general, when the energy deposited in the molecule becomes high enough, as in QCMD, the downshifts could be captured, at least partially, because the trajectories start to sample the anharmonic region of the potential energy surface, as was shown in the QCMD spectrum of HONO in ref. 10. A possible explanation is that due to the strong coupling, the energy leakage from the high-frequency stretches is very fast, and so the actual energy in these stretches is still small even in QCMD. Note that while the MD O-H band is centered at the harmonic frequency, the band is broadened compared to the double harmonic stick shown in Figure 1, whereas other MD bands remain sharp. We speculate that this is due to strong perturbations of the O-H motion from the intermolecular modes.

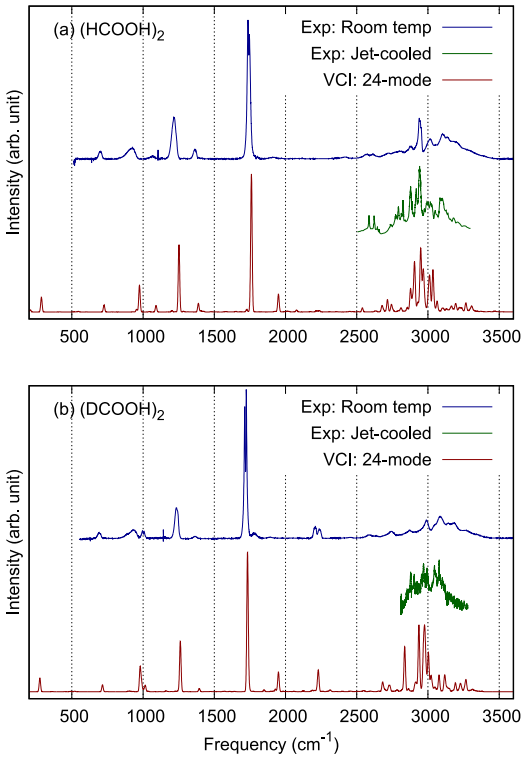

Fig. 4 Comparison of the room-temperature experimental spectrum, the jet-cooled spectrum, and the theoretical one, for (a) $(HCOOH)_2$ and (b) $(DCOOH)_2$.

In QCMD calculations, double-proton transfer was observed for $(HCOOH)_2$ and $(DCOOH)_2$, but these are relatively rare (about 10% of the trajectories). In addition, when we included those proton transfer trajectories for the computations of the spectrum, the spectra are basically the same as the ones shown in Figure 3 that were obtained using all the trajectories. These observations indicate that the complexity of the band is not due to the proton transfer motion that visits both wells. In addition, our VSCF/VCI calculations (see below) also support this conclusion, since the complexity of the O-H stretch band can be well reproduced by these calculations that were restricted in a single minimum well. Finally, we note the 7-mode wavepacket calculations by Luckhaus,[44] who determined the splitting for vibrationally excited states of FAD and reported values much less than 1 cm^{-1}, which clearly indicates localization of the wavefunctions. So, at the level of resolution of both theory and experiment shown here, neglecting double-proton transfer is justified.

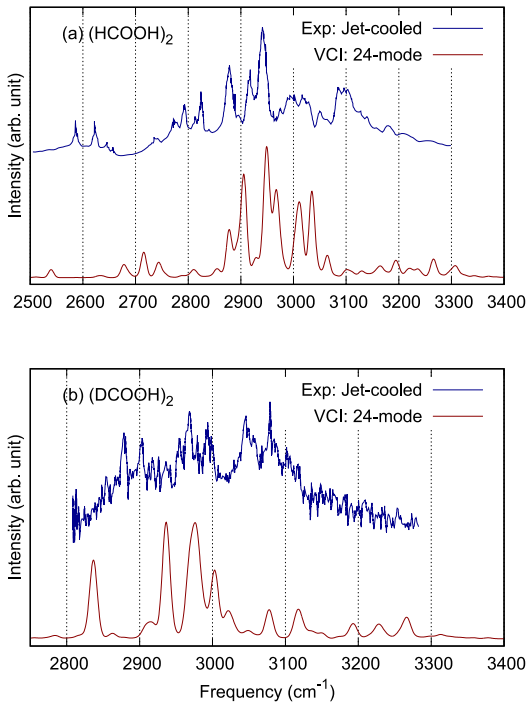

Fig. 5 Comparison between the jet-cooled and theoretical IR spectra of $(HCOOH)_2$ and $(DCOOH)_2$ for the O-H stretch band.

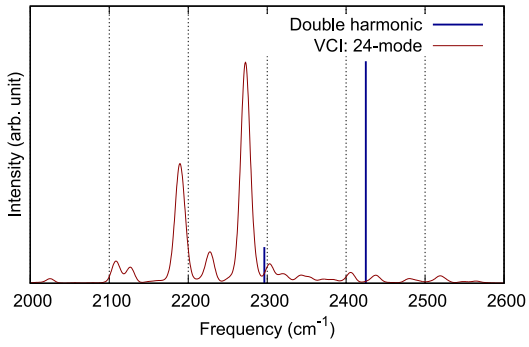

Fig. 6 Theoretical IR spectrum of $(DCOOD)_2$ for the C-D and O-D stretch bands.

Next we compare the quantum spectra with the experimental ones. Figure 4 shows the room-temperature, jet-cooled, and the VSCF/VCI spectra of $(HCOOH)_2$ and $(DCOOH)_2$. Although the spectra produced from VSCF/VCI calculations are at 0 K and $J = 0$, they still agree well with the room-temperature survey spectra. For the stretch bands, the experimental spectra at room

temperature have low resolution, so we compare our theoretical stretch bands with the jet-cooled experiments instead, which is shown in Figure 5. According to our VSCF/VCI calculations, the O-H stretch bands of the $(HCOOH)_2$ and $(DCOOH)_2$ are complex, due to the strong coupling. A detailed analysis of this band will be given below. For $(HCOOH)_2$, our VSCF/VCI spectrum aligns reasonably well with the jet-cooled experiment, with the most intense transition at about 2950 cm^{-1}, which is the C-H stretch, but strongly coupled with the O-H stretch that carries large intensity. For $(DCOOH)_2$, the C-D stretch moves to around 2250 cm^{-1}, so only the O-H stretch band is in this spectral range. Yet we find this band still very complex, owing to the coupling between the OH stretch with many low-frequency modes. The experimental jet-cooled spectrum for this isotopologue is very noisy, making it difficult to compare our theory with experiment. Nevertheless, the agreement is reasonably good. The VSCF/VCI calculation is able to reproduce the correct spectral shift (about 300 cm^{-1}) and the complexity and width of this O-H stretch band, though quantitative agreement with experiment is not achieved. For $(DCOOD)_2$, the IR spectrum in the C-D and O-D stretch region is shown in Figure 6; however, only the Raman spectrum has been measured experimentally[25] so that there would not be direct comparison between our theory and the experiment. Similar to the Raman spectrum, the O-D stretch band of $(DCOOD)_2$ is significantly sharper than the OH bands of $(HCOOH)_2$ and $(DCOOH)_2$, but it is still more complex than the double harmonic spectrum, which only has two transitions in this spectral range.

The assignment of this complex O-H stretch band is clearly problematic because of the massive coupling in this spectral range. In order to further characterize the eigenstates obtained in the VSCF/VCI calculations, we analyzed the CI coefficients for the three isotopologues. The VSCF/VCI calculations provide the CI coefficients of the basis for each molecular eigenstate (see eqn. 4). In the usual approach, we examine the dominant CI coefficient for each bright state and thereby make the "assignment." However, in the present 24-mode calculations, since many zeroth order states contribute to a molecular eigenstate and there is not a dominant coefficient, such an analysis is not illuminating, except to note that these coefficients are all relatively small. Therefore, we present a graphical representation of this analysis for the three isotopologues instead. Specifically, in Figure 7, we plot the sum of the squares of the VCI coefficients of the C-H(D) and O-H(D) stretches in 20 cm^{-1}-windows, as a function of eigenenergy across the band. One can immediately see that for $(HCOOH)_2$ (panel a), the OH stretch coefficients are widely spread all over the band, and all these coefficients are small. Therefore, it's essentially impossible to assign a certain range to the OH stretch. On the other hand, in $(HCOOH)_2$, though there are also several states with significant coefficient for the C-H stretch, it is less diluted, and most of them cluster between 2900 and 3000 cm^{-1}, so we could assign this range to the C-H stretch, which agrees with the conclusion from isotopic substitution experiment.[21] Note that the zeroth order O-H stretch mixes with these states, and this explains the large intensity of the band at about 2950 cm^{-1} in the VSCF/VCI spectrum. In $(DCOOH)_2$ (panel b), the C-D stretch shifts to about 2240 cm^{-1} due to deuteration, and it looks like a

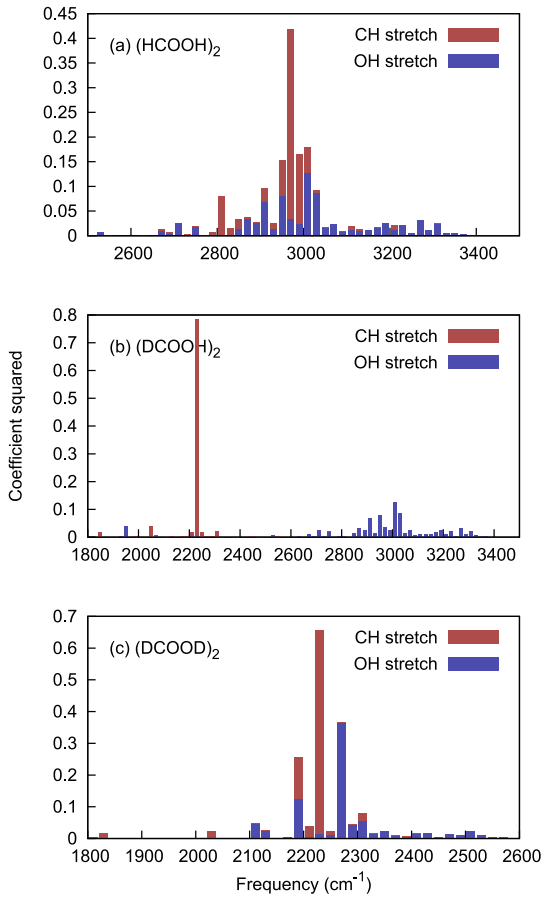

Fig. 7 Square of the VCI coefficients of the C-H(D) and O-H(D) stretches as a function of energy across the O-H stretch band for: (a) $(HCOOH)_2$, (b) $(DCOOH)_2$, and (c) $(DCOOD)_2$.

pure state. However, in fact there is a doublet due to the coupling between the C-D fundamental and the combination mode of the C-O single-bond stretch and C-D in-plane bend; in our histogram graph that utilized a window of a 20 cm^{-1} width, this cannot be resolved. The O-H stretch, however, still spreads across the band, even though it does not couple with the CD stretch. The O-H stretch in both $(HCOOH)_2$ and $(DCOOH)_2$ couples strongly with the low-frequency modes. A visualization of the normal modes of FAD can be found in the supplementary material of ref. 47. Specifically, the modes that can strongly perturb the hydrogen bonds such as the dimer stretch (mode 4), the out-of-plane wag of the dimer (mode 3, 5), the O–C=O bend (mode 7, 8), and in-plane rock of the dimer (mode 2, 6), contributes a lot in those overtones and combination modes that directly couple with the OH stretch. Lastly, for $(DCOOD)_2$ (panel c), both C-D and O-D stretch bands are relatively less complex: the transition at about 2230 cm^{-1} is the C-D stretch, and the transition at about 2270 cm^{-1} is the O-D stretch. The peak at about 2190 cm^{-1} is a strongly mixed one, but with significant contribution from both the zeroth order C-D and O-D stretches.

4 Summary and Conclusions

We reported quantum and molecular dynamics calculations of the IR spectra of formic acid dimer, $(HCOOH)_2$, and two isotopologues, $(DCOOH)_2$ and $(DCOOD)_2$ using recent full dimensional, *ab initio* potential energy and dipole moment surfaces. The quantum calculations considered all 24 normal modes; this was made feasible by using a 4-mode representation of the full potential and a 3-mode representation of the dipole moment surface. The three IR spectra are all display a complex band in the nominally assigned O-H or O-D stretch region, in accord with experimentally measured bands in the IR spectra of $(HCOOH)_2$ and $(DCOOH)_2$ and the Raman spectrum of $(DCOOD)_2$. In the case of $(DCOOD)_2$ the band is sharper than the higher-energy O-H stretch band. Other calculated bands are relatively "simple" and easily assigned. Indeed, the double harmonic approximation, using the PES and DMS, accounts reasonably well for these low-frequency experimental bands. Overall, the comparison between the quantum and experimental spectra is of unprecedented accuracy, although quantitative differences exist. This may be due to some deficiencies in the PES. For example, the harmonic frequency of the IR-active O-H stretch differs from the benchmark one[57] by 20 cm^{-1}. The MD calculations of the IR spectra of $(HCOOH)_2$ and $(DCOOH)_2$ show good agreement with the quantum ones and experiment, with the exception of the complex bands mentioned already. While the MD band is complex, the band center is upshifted by roughly 300 cm^{-1} relative to experiment and also the quantum band centers for $(HCOOH)_2$ and $(DCOOH)_2$. We ascribe this the usual difficulty in MD simulations to fully capture the positive anharmonicity of X-H stretches. Nevertheless, it may appear that the MD method is correct in capturing the complexity of this band. However, this conclusion has to be made with caution. Complexity in MD bands is not necessarily correct. The evidence for this is the comparison of the 0 K QCMD (which we remind the reader these authors term as "semi-classically prepared MD") IR spectrum of HONO with the accurate quantum one using a realistic PES and DMS.[10] In this case the quantum band for the O-H stretch is essentially a stick located at 3590 cm^{-1} while the 0 K QCMD band is broad (roughly 100 cm^{-1} width) with the band center at approximately 3670 cm^{-1}. No analysis of the cause of this broadening was made in that paper, so we can only speculate that perhaps some of internal energy may have "leaked" to the isomerization coordinate. In general though it is known that intensities from MD calculations are often not reliable, quoting from ref. 10 "The present results highlight the difficulty of calculating accurate intensities from molecular dynamics, even with trajectories longer than 100 ps."

The present calculations also have important conclusions about the recent the MD calculations of the IR spectrum of $(HCOOH)_2$ and $(DCOOH)_2$ described in the Introduction by the theoretical group of Meuwly and co-workers.[24] As noted already, this procedure assumes that the MD approach to calculate at least the position of the complex O-H stretch is accurate and thus can be used to modify a PES to obtain a presumably reliable estimate of, in this case, the barrier to double proton transfer. Based on the results of the comparison of the MD and quantum spectra here for FAD, we conclude that this assumption is not valid. Thus, the reported estimate of the barrier heights is not reliable. Indeed, th barrier height of the PES used here, 8.2 kcal/mol, and reported in earlier CCSD(T) calculations of Marx and co-workers[45] is the reliable one. We speculate that the decrease in barrier height actually results in a significant decrease of the O-H harmonic frequency, which then can tune the resulting MD O-H stretch band to agree with experiment.

5 Acknowledgments

We thank the National Science Foundation for financial support.

References

1 J. M. Bowman, T. Carrington and H.-D. Meyer, *Mol. Phys.*, 2008, **106**, 2145–2182.
2 O. Christiansen, *Phys. Chem. Chem. Phys.*, 2012, **14**, 6672–6687.
3 A. G. Csaszar, C. Fabri, T. Szidarovszky, E. Matyus, T. Furtenbacher and G. Czako, *Phys. Chem. Chem. Phys.*, 2012, **14**, 1085–1106.
4 J. Tennyson, *J. Chem. Phys.*, 2016, **145**, 120901.
5 T. C. Jr., *J. Chem. Phys.*, 2017, **146**, 120902.
6 C. Qu, Q. Yu and J. M. Bowman, *Annu. Rev. Phys. Chem.*, 2018, **69**, 6.1–6.25.
7 X. Huang, B. J. Braams and J. M. Bowman, *J. Chem. Phys*, 2005, **122**, 044308.
8 B. J. Braams and J. M. Bowman, *Int. Rev. Phys. Chem.*, 2009, **28**, 577–606.
9 A. Witt, S. D. Ivanov, M. Shiga, H. Forbert and D. Marx, *J. Chem. Phys.*, 2009, **130**, 194510.
10 N.-T. Van-Oanh, C. Falvo, F. Calvo, D. Lauvergnat, M. Basire, M.-P. Gaigeot and P. Parneix, *Phys. Chem. Chem. Phys.*, 2012, **14**, 2381–2390.
11 M. Thomas, M. Brehm, R. Fligg, P. Vohringer and B. Kirchner, *Phys. Chem. Chem. Phys.*, 2013, **15**, 6608–6622.
12 D. R. Galimberti, A. Milani, M. Tommasini, C. Castiglioni and M.-P. Gaigeot, *J. chem. Theory Comput.*, 2017, **13**, 3802–3813.
13 J. M. Bowman, *J. Chem. Phys.*, 1978, **68**, 608.
14 K. M. Christoffel and J. M. Bowman, *Chem. Phys. Lett.*, 1982, **85**, 220.
15 S. Carter, S. J. Culik and J. M. Bowman, *J. Chem. Phys.*, 1997, **107**, 10458–10469.
16 J. M. Bowman, S. Carter and X. Huang, *Int. Rev. Phys. Chem.*, 2003, **22**, 533.
17 X. Wang, S. Carter and J. M. Bowman, *J. Phys. Chem. A*, 2015, **119**, 11632–11640.
18 Ö. Birer and M. Havenith, *Annu. Rev. Phys. Chem.*, 2009, **60**, 263–275.
19 Y. Zhang, W. Li, W. Luo, Y. Zhu and C. Duan, *J. Chem. Phys.*, 2017, **146**, 244306.
20 F. Ito and T. Nakanaga, *Chem. Phys. Lett.*, 2000, **318**, 571–577.

21 F. Ito and T. Nakanaga, *Chem. Phys.*, 2002, **277**, 163–169.
22 R. Georges, M. Freytes, D. Hurtmans, I. Kleiner, J. Vander Auwera and M. Herman, *Chem. Phys.*, 2004, **305**, 187–196.
23 M. W. Nydegger, W. Rock and C. M. Cheatum, *Phys. Chem. Chem. Phys.*, 2011, **13**, 6098–6104.
24 K. Mackeprang, Z. H. Xu, Z. Maroun, M. Meuwly and H. G. Kjaergaard, *Phys. Chem. Chem. Phys.*, 2016, **18**, 24654–24662.
25 P. Zielke and M. A. Suhm, *Phys. Chem. Chem. Phys.*, 2007, **9**, 4528–4534.
26 G. M. Florio, T. S. Zwier, E. M. Myshakin, K. D. Jordan and E. L. Sibert, *J. Chem. Phys.*, 2003, **118**, 1735–1746.
27 Z. Xue and M. A. Suhm, *J. Chem. Phys.*, 2009, **131**, 054301.
28 G. L. Barnes and E. L. Sibert, *J. Mol. Spectrosc.*, 2008, **249**, 78–85.
29 Y. H. Yoon, M. L. Hause, A. S. Case and F. F. Crim, *J. Chem. Phys.*, 2008, **128**, 084305.
30 N. Shida, P. F. Barbara and J. E. Almlöf, *J. Chem. Phys.*, 1991, **94**, 3633.
31 Y. Kim, *J. Am. Chem. Soc.*, 1996, **118**, 1522–1528.
32 T. Loerting and K. R. Liedl, *J. Am. Chem. Soc.*, 1998, **120**, 12595–12600.
33 S. Miura, M. E. Tuckerman and M. L. Klein, *J. Chem. Phys.*, 1998, **109**, 5290–5299.
34 M. V. Vener, O. Kühn and J. M. Bowman, *Chem. Phys. Lett.*, 2001, **349**, 562–570.
35 H. Ushiyama and K. Takatsuka, *J. Chem. Phys.*, 2001, **115**, 5903–5912.
36 C. S. Tautermann, A. F. Voegele and K. R. Liedl, *J. Chem. Phys.*, 2004, **120**, 631.
37 Z. Smedarchina, A. Fernández-Ramos and W. Siebrand, *Chem. Phys. Lett.*, 2004, **395**, 339–345.
38 P. R. L. Markwick, N. L. Doltsinis and D. Marx, *J. Chem. Phys.*, 2005, **122**, 054112.
39 F. Fillaux, *Chem. Phys. Lett.*, 2005, **408**, 302–306.
40 G. V. Mil'nikov, O. Kühn and H. Nakamura, *J. Chem. Phys.*, 2005, **123**, 074308.
41 D. Luckhaus, *J. Phys. Chem. A*, 2006, **110**, 3151–3158.
42 C. Burisch, P. R. L. Markwick, N. L. Doltsinis and J. Schlitter, *J. Chem. Theory Comput.*, 2008, **4**, 164–172.
43 I. Matanović, N. Došlić and B. R. Johnson, *J. Chem. Phys.*, 2008, **128**, 084103.
44 D. Luckhaus, *Phys. Chem. Chem. Phys.*, 2010, **12**, 8357–8361.
45 S. D. Ivanov, I. M. Grant and D. Marx, *J. Chem. Phys.*, 2015, **143**, 124304.
46 A. Jain and E. L. Sibert, *J. Chem. Phys.*, 2015, **142**, 084115.
47 C. Qu and J. M. Bowman, *Phys. Chem. Chem. Phys.*, 2016, **18**, 24835.
48 J. O. Richardson, *Phys. Chem. Chem. Phys.*, 2017, **19**, 966–970.
49 Y.-T. Chang, Y. Yamaguchi, W. H. Miller and H. F. Schaefer, *J. Am. Chem. Soc.*, 1987, **109**, 7245–7253.
50 I. Matanović and N. Došlić, *Chem. Phys.*, 2007, **338**, 121–126.
51 G. A. Pitsevich, A. E. Malevich, E. N. Kozlovskaya, I. Y. Doroshenko, V. Sablinskas, V. Pogorelov, D. Dovgal and V. Balevicius, *Vib. Spectrosc.*, 2015, **79**, 67–75.
52 C. Qu and J. M. Bowman, *J. Chem. Phys.*, 2018, **148**, 241713.
53 J. K. G. Watson, *Mol. Phys.*, 1968, **15**, 479.
54 T. Esser, H. Knorke, R. Asmis, Knut, W. Schöllkopf, Q. Yu, C. Qu, M. Bowman, Joel and M. Kaledin, *J. Phys. Chem. Lett.*, 2018, **9**, 798–803.
55 W. L. Hase, in *Encyclopeida of Computational Chemistry*, ed. N. L. Allinger, Wiley: New York, 1998, vol. 1, pp. 399–407.
56 I. Reva, A. Plokhotnichenko, E. Radchenko, G. Sheina and Y. Blagoi, *Spectrochim. Acta A*, 1994, **50**, 1107 – 1111.
57 E. Miliordos and S. S. Xantheas, *J. Chem. Phys.*, 2015, **142**, 094311.

Full-dimensional (24 modes) quantum calculation of the IR spectrum of $(DCOOD)_2$, and comparison with classical MD one.